

## To-do list

Fix the notation:

- $m = 1, \dots, N$ : position
- $n = 1, \dots, N$ : energy eigenvalue.

Fix the notation: use a single index  $j$  instead of two separate indices for site and spin, except where absolutely necessary.

Fix the notation:  $|001\rangle = \hat{d}_1 |0\rangle$  or  $|001\rangle = \hat{d}_3 |0\rangle$ ?

Fix the notation: be consistent in the order of creation/annihilation operators in the hopping and Cooper pair creation/breaking terms.

Spin rotation invariance puts us in a different symmetry class.



# Chapter 1

## Superconductors can be described by single-particle Hamiltonians

In the first semester, we used single-particle quantum mechanics to learn that topological insulators host protected edge states. In the Su-Schrieffer-Heeger model, these are bound states whose energy is pinned at 0. In 2-dimensional topological insulators (e.g., the Qi-Wu-Zhang model or the Bernevig-Hughes-Zhang model), edge states form bands which allow for perfect (reflectionless, zero four-terminal resistance) conduction. Real materials contain many electrons, but since the Hamiltonians of topological insulators preserve the particle number and do not include electron-electron interactions, we could obtain the true ground state by just filling all negative energy eigenstates by one electron.

This semester, we study topological superconductors. Here the electrons are in contact with a reservoir of Cooper pairs, which we will treat in the mean-field approximation. Cooper pair formation and Cooper pair breaking will be included in the Hamiltonian as pairs of electrons disappearing from the system, or added to the system, coherently. Particle number is no longer conserved, and a straightforward description of the system by a single-particle Hamiltonian is not possible.

There is a way to associate a single-particle Hamiltonian to a superconductor, known as the Bogoliubov-de Gennes trick. Because it is not entirely trivial to interpret its results, we dedicate the first few lessons to this formalism.

### 1.1 The Kitaev Wire Hamiltonian

The Kitaev wire is a toy model for a  $p$ -wave superconducting wire. It describes spinless fermions (e.g., spin polarized electrons) hopping on a chain consisting of  $N$  sites. The chain lies on top of a superconductor, which has a condensate

of Cooper-pairs. Thus, pairs of electrons on neighboring sites can hop off the chain simultaneously and form a Cooper pair in the superconductor. The inverse process can also occur: a Cooper pair in the superconductor can be broken, if the resulting fermions both end up in the chain, on neighboring sites. The grand canonical Hamiltonian of this system reads,

$$\hat{H}_K = \sum_{m=1}^N u_m \hat{c}_m^\dagger \hat{c}_m + \sum_{m=1}^{N-1} (t_m \hat{c}_m^\dagger \hat{c}_{m+1} + h.c.) + \sum_{m=1}^{N-1} (\Delta_m^* \hat{c}_m \hat{c}_{m+1} + h.c.). \quad (1.1)$$

The operator  $\hat{c}_m$  annihilates an electron from site  $m$ . The first term describes the onsite potentials  $u_m$ , which includes the chemical potential plus any site-dependent terms (e.g., electric potential from back-gates). The second term is the hopping of electrons between neighboring sites, with position-dependent amplitude  $t_m$ . The last term is the effect of superconductivity in the mean-field approximation, via the pair potential  $\Delta_m$ , a set of complex parameters, corresponding to the wave function of the Cooper pair condensate. To calculate  $\Delta_m$  self-consistently, we would need a description of the bulk superconductor, but in these notes, as in a large part of the literature, we treat  $\Delta_m$  as parameters with no dynamics. In most of this chapter we will study the homogeneous case, with position independent hopping amplitude  $t_m = t$  and pair potential  $\Delta_m = \Delta$ .

## 1.2 Fock space

The Kitaev wire, like all superconducting models, does not conserve the particle number. Therefore, the dynamics it describes takes place in the Fock space.

### 1.2.1 Computational basis notation

A set of  $2^N$  basis states that spans the Fock space can be defined using the operators  $\hat{c}_m$ . We start with the state  $|\emptyset\rangle$  of the system with no particles present,

$$\hat{c}_m |\emptyset\rangle = 0 \quad \text{for } m = 1, \dots, N. \quad (1.2)$$

We then specify for each site  $m$  whether it is occupied or not. In the case of  $N = 3$  sites, the set of basis states reads

$$\begin{aligned} |000\rangle &= |\emptyset\rangle; & |100\rangle &= \hat{c}_1^\dagger |\emptyset\rangle; & |010\rangle &= \hat{c}_2^\dagger |\emptyset\rangle; & |110\rangle &= \hat{c}_2^\dagger \hat{c}_1^\dagger |\emptyset\rangle; \\ |001\rangle &= \hat{c}_3^\dagger |\emptyset\rangle; & |101\rangle &= \hat{c}_3^\dagger \hat{c}_1^\dagger |\emptyset\rangle; & |011\rangle &= \hat{c}_3^\dagger \hat{c}_2^\dagger |\emptyset\rangle; & |111\rangle &= \hat{c}_3^\dagger \hat{c}_2^\dagger \hat{c}_1^\dagger |\emptyset\rangle. \end{aligned}$$

Note that the order of the operators is important, e.g.,

$$|010\rangle = -\hat{c}_1 |110\rangle = \hat{c}_3 |001\rangle. \quad (1.3)$$

### 1.2.2 Matrices for the operators

Describe the construction of the matrix of fermion operators  $\hat{c}_m$ .  
Build the matrix of the Hamiltonian  $\hat{H}_K$ .

### 1.2.3 Example: two-site wire

As an illustrative case, we consider the simplest example, the Kitaev wire on  $N = 2$  sites. The Hamiltonian reads

$$\hat{H}_K = u_1 \hat{c}_1^\dagger \hat{c}_1 + u_2 \hat{c}_2^\dagger \hat{c}_2 + t \hat{c}_1^\dagger \hat{c}_2 + t \hat{c}_2^\dagger \hat{c}_1 + \Delta \hat{c}_2^\dagger \hat{c}_1^\dagger + \Delta^* \hat{c}_1 \hat{c}_2. \quad (1.4)$$

For such a small system, we can actually calculate everything in the Hilbert space of all states:

$$\hat{H} = \begin{pmatrix} |00\rangle & |01\rangle & |10\rangle & |11\rangle \end{pmatrix} \begin{pmatrix} 0 & 0 & 0 & \Delta^* \\ 0 & u_2 & t & 0 \\ 0 & t & u_1 & 0 \\ \Delta & 0 & 0 & u_1 + u_2 \end{pmatrix} \begin{pmatrix} \langle 00| \\ \langle 01| \\ \langle 10| \\ \langle 11| \end{pmatrix} \quad (1.5)$$

$$(1.6)$$

The spectrum of  $\hat{H}$ , shown in Fig., is symmetric around  $E = -\mu$ . This symmetry has nothing to do with superconductivity, it is a generic feature of free Hamiltonians (i.e., where  $\hat{H}$  is a quadratic function of the operators  $\hat{c}_m$  and  $\hat{c}_m^\dagger$ ), which can be explained simply. All energy levels can be obtained from the bottom up, starting with  $|GS\rangle$ , and adding particles  $\hat{d}$ , as indicated by the slashed lines. Alternatively, one can go top-down: with the state where all  $d$  fermions are present, and subtract the  $\hat{d}$ 's. The symmetry point can be shifted by onsite potentials, but is always there. We will now describe a systematic way to obtain the operators  $\hat{d}$

## 1.3 The ground state of a mean-field superconductor can be constructed from its normal modes

In the mean-field approximation, a superconductor such as the Kitaev wire is described by a free Hamiltonian, i.e., quadratic in the electron creation and annihilation operators. Note that although the number of fermions is not conserved, the parity is. Since this is a free Hamiltonian (quadratic), it can be diagonalized by introducing new fermionic operators,

$$\hat{d}_n = \sum_m u_{nm} \hat{c}_m + v_{nm} \hat{c}_m^\dagger; \quad \hat{d}_n^\dagger = \sum_m u_{nm}^* \hat{c}_m^\dagger + v_{nm}^* \hat{c}_m. \quad (1.7)$$

We require that the  $\hat{d}_n$  obey fermionic commutation relations,

$$\{\hat{d}_n, \hat{d}_l\} = 0; \quad \{\hat{d}_n, \hat{d}_l^\dagger\} = \delta_{nl}. \quad (1.8)$$

What requirements do the commutation relations impose on the coefficients  $u_{nm}$  and  $v_{nm}$ ?

These particles diagonalize the Hamiltonian in the sense that

$$\hat{H} = \sum_{n=1}^N E_n \hat{d}_n^\dagger \hat{d}_n + \text{const.} \quad (1.9)$$

This looks very much like the standard procedure for free Hamiltonians, however, because of the superconducting pair potential,  $\Delta$ , we cannot take  $\hat{d}_n$  to be a linear combination of only electron annihilation operators,  $\hat{c}_m$ . This means that  $\hat{d}_n$  and  $\hat{d}_n^\dagger$  are described on the same footing. We will use this freedom to ensure that all of the  $\hat{d}$  operators describe positive energy excitations:

$$E_n \geq 0 \quad \text{for } n = 1, \dots, N. \quad (1.10)$$

This can be achieved by redefining the negative energy fermions  $\hat{d}_n$  as  $\hat{d}_n \leftrightarrow \hat{d}_n^\dagger$ .

Once we have found the operators  $\hat{d}_n$ , we can construct the Ground State  $|GS\rangle$  of the Hamiltonian. This is the vacuum of the operators  $\hat{d}_n$ , i.e.,

$$\forall l = 1, \dots, N : \hat{d}_l |GS\rangle = 0. \quad (1.11)$$

The ground state is a complicated state when expressed in the basis of the original fermions  $\hat{c}_m$ : it is in general a superposition of states with different particle numbers, since the Hamiltonian does not conserve particle number. However, since the Hamiltonian conserves the parity of the particle number, the ground state is a superposition of states with only odd, or only even number of particles ( $\hat{c}_m$  fermions).

One way to construct the ground state  $|GS\rangle$  is to turn the logic of the previous paragraph around. Starting from any “seed” state, we can proceed to take away all the components of it that contain excitations  $\hat{d}$ : then we are left with  $|GS\rangle$ , if the seed state had a  $|GS\rangle$  component. A frequent choice for the seed state is  $|00\dots 0\rangle$ , the vacuum of the  $\hat{c}_m$  fermions, which gives

$$\hat{d}_N \hat{d}_{N-1} \dots \hat{d}_1 |\emptyset\rangle \propto |GS\rangle \text{ or } 0. \quad (1.12)$$

If the initial state had no component of the ground state (because, e.g., the ground state is odd), we can continue this procedure with other seed states.<sup>1</sup>

<sup>1</sup>Alternatively, the projector to the ground state can be obtained if we remove all single-particle excitations from the mixture of all possible states,

$$|GS\rangle \langle GS| = \hat{d}_N \hat{d}_{N-1} \dots \hat{d}_1 \left( \sum_{n_1=0}^1 \dots \sum_{n_N=0}^1 \hat{c}_N^{\dagger n_N} \dots \hat{c}_1^{\dagger n_1} |0\rangle \langle 0| \hat{c}_1^{n_1} \dots \hat{c}_N^{n_N} \right) \hat{d}_1^\dagger \hat{d}_2^\dagger \dots \hat{d}_N^\dagger. \quad (1.13)$$

### 1.3.1 Using the eigenmodes, we can construct the whole spectrum

If we have the ground state  $|GS\rangle$  and the eigenmodes  $\hat{d}_n$  of the Hamiltonian, we can construct all  $2^N$  of its eigenstates. We simply specify which of the  $\hat{d}_m$  fermions are present in the system, e.g.,

$$|000\dots 0\rangle_d = |GS\rangle; \quad |100\dots 0\rangle_d = \hat{d}_1^\dagger |GS\rangle \quad (1.14)$$

$$|010\dots 0\rangle_d = \hat{d}_2^\dagger |GS\rangle; \quad |110\dots 0\rangle_d = \hat{d}_2^\dagger \hat{d}_1^\dagger |GS\rangle. \quad (1.15)$$

## 1.4 The normal modes of a mean-field superconductor are obtained by diagonalizing the Bogoliubov–de Gennes Hamiltonian

We have shown how to construct eigenstates of the superconductor if the coefficients  $u_{n,j}, v_{n,j}$  of Eq. (1.7) are found. There is a trick to obtain these, called the Bogoliubov–de Gennes formalism, that involves a redundant representation of the states.

We begin by symmetrizing each term in the Hamiltonian. We use the fermionic anticommutation relations, whereby,

$$\hat{c}_m \hat{c}_j = \frac{1}{2} \hat{c}_m \hat{c}_j - \frac{1}{2} \hat{c}_j \hat{c}_m; \quad \hat{c}_m^\dagger \hat{c}_j = \frac{1}{2} \hat{c}_m^\dagger \hat{c}_j - \frac{1}{2} \hat{c}_j \hat{c}_m^\dagger + \frac{1}{2} \delta_{mj}; \quad (1.16a)$$

$$\hat{c}_m^\dagger \hat{c}_j^\dagger = \frac{1}{2} \hat{c}_m^\dagger \hat{c}_j^\dagger - \frac{1}{2} \hat{c}_j^\dagger \hat{c}_m^\dagger; \quad \hat{c}_m \hat{c}_j^\dagger = \frac{1}{2} \hat{c}_m \hat{c}_j^\dagger - \frac{1}{2} \hat{c}_j^\dagger \hat{c}_m + \frac{1}{2} \delta_{mj}. \quad (1.16b)$$

We substitute these into the Hamiltonian, to obtain its symmetrized form,

$$\hat{H} = \frac{1}{2} \sum_{j,m=1}^N \left( h_{mj} (\hat{c}_m^\dagger \hat{c}_j - \hat{c}_j \hat{c}_m^\dagger) + \Delta_{mj} \hat{c}_m^\dagger \hat{c}_j^\dagger + \Delta_{mj}^* \hat{c}_j \hat{c}_m \right) + \frac{1}{2} \sum_{m=1}^N h_{mm}. \quad (1.17)$$

The complex numbers  $h_{mj}$  and  $\Delta_{mj}$ , read out from the Hamiltonian, are grouped into matrices. Hermiticity of the Hamiltonian ensures that the matrix  $h$  is Hermitian, while the symmetrization, Eq. (1.16), ensures that the matrix  $\Delta$  is antisymmetric, i.e.,

$$h_{jm} = h_{mj}^*; \quad \Delta_{jm} = -\Delta_{mj}. \quad (1.18)$$

As an example, for the Kitaev wire, Eq. (1.1), on  $N = 4$  sites, the matrices  $h$  and  $\Delta$  read,

$$h = \begin{pmatrix} u_1 & t_1 & 0 & 0 \\ t_1 & u_2 & t_2 & 0 \\ 0 & t_2 & u_3 & t_3 \\ 0 & 0 & t_3 & u_4 \end{pmatrix}; \quad \Delta = \begin{pmatrix} 0 & -\Delta_1 & 0 & 0 \\ \Delta_1 & 0 & -\Delta_2 & 0 \\ 0 & \Delta_2 & 0 & -\Delta_3 \\ 0 & 0 & \Delta_3 & 0 \end{pmatrix}; \quad (1.19)$$

Using a practical shorthand,

$$\hat{\mathbf{c}}^\dagger = (\hat{c}_1^\dagger, \hat{c}_2^\dagger, \dots, \hat{c}_N^\dagger), \quad (1.20)$$

the Hamiltonian can be written in a compact form as

$$\hat{H} = \frac{1}{2} \begin{pmatrix} \hat{\mathbf{c}}^\dagger & \hat{\mathbf{c}} \end{pmatrix} \mathcal{H} \begin{pmatrix} \hat{\mathbf{c}} \\ \hat{\mathbf{c}}^\dagger \end{pmatrix} + \frac{1}{2} \text{Tr} h; \quad \mathcal{H} = \begin{pmatrix} h & \Delta \\ -\Delta^* & -h^* \end{pmatrix}. \quad (1.21)$$

The matrix  $\mathcal{H}$  is known as the Bogoliubov-de Gennes (BdG) Hamiltonian. Because of the symmetrization procedure, the BdG Hamiltonian has particle-hole symmetry (PHS), represented by  $\sigma_x K$ , i.e.,

$$\sigma_x = \begin{pmatrix} 0 & \mathbb{I} \\ \mathbb{I} & 0 \end{pmatrix}; \quad \sigma_x \mathcal{H}^* \sigma_x = -\mathcal{H}. \quad (1.22)$$

Due to the particle-hole symmetry of  $\mathcal{H}$ , we can diagonalize it using only the positive energy eigenstates,

$$\mathcal{H} \begin{pmatrix} u_n^* \\ v_n^* \end{pmatrix} = E_n \begin{pmatrix} u_n^* \\ v_n^* \end{pmatrix}, \quad \text{with } E_n \geq 0 \text{ for } n = 1, \dots, N; \quad (1.23)$$

$$\mathcal{H} \begin{pmatrix} v_n \\ u_n \end{pmatrix} = -E_n \begin{pmatrix} v_n \\ u_n \end{pmatrix}, \quad \text{for } n = 1, \dots, N, \quad (1.24)$$

where the  $n$ th eigenvector of  $\mathcal{H}$  was written as  $(u_n, v_n)^\dagger$ , with  $u_n$  and  $v_n$  both  $N$ -component vectors. Remember that  $\mathcal{H}$  was a Hermitian matrix, and thus its eigenvectors form an orthonormal basis.

We can use the components  $u_{nm}$  and  $v_{nm}$  to define new operators as per Eq. (1.7),

$$\hat{d}_n = \sum_m u_{nm} \hat{c}_m + v_{nm} \hat{c}_m^\dagger; \quad \hat{d}_n^\dagger = \sum_m u_{nm}^* \hat{c}_m^\dagger + v_{nm}^* \hat{c}_m. \quad (1.25)$$

Orthonormality of the eigenvectors translates to the required anticommutation relations.

We can check that the fermions introduced above really are the eigenmodes of the Hamiltonian. We can write  $\mathcal{H}$  as

$$\mathcal{H} = \sum_n E_n \begin{pmatrix} u_n^* \\ v_n^* \end{pmatrix} \begin{pmatrix} u_n & v_n \end{pmatrix} - \sum_n E_n \begin{pmatrix} v_n \\ u_n \end{pmatrix} \begin{pmatrix} v_n^* & u_n^* \end{pmatrix}. \quad (1.26)$$

Comparing this with Eq. (1.21), we find that it corresponds to

$$\hat{H} = \frac{1}{2} \sum_{n=1}^N E_n (\hat{d}_n^\dagger \hat{d}_n - \hat{d}_n \hat{d}_n^\dagger) + \frac{1}{2} \sum_{n=1}^N E_n = \sum_{n=1}^N E_n \hat{d}_n^\dagger \hat{d}_n, \quad (1.27)$$

the form that we were looking for.

## Chapter 2

# The Kitaev Wire is mapped to the SSH model using Majorana Fermions

The Kitaev wire is a superconducting chain of  $N$  spinless fermions. Its many-body Hamiltonian reads

$$\hat{H} = \sum_j V_j \hat{c}_j^\dagger \hat{c}_j + \sum_j \left( \Delta_j^* \hat{c}_{j+1} \hat{c}_j - t_j \hat{c}_j^\dagger \hat{c}_{j+1} + h.c. \right). \quad (2.1)$$

Using the BdG trick we associate a  $2N \times 2N$  Hamiltonian to the Kitaev wire. As we show in this chapter, this maps onto the SSH model using Majorana fermion operators.

### 2.1 The Kitaev Wire and the SSH model are in the same universality class

The fundamental symmetries of the Kitaev wire and the SSH model are listed in Table 2.1. They are the same, so we expect that the BdG Hamiltonian of the Kitaev wire can host robust edge states.

#### 2.1.1 The mapping is made explicit by a basis transformation

To map the Kitaev wire onto the SSH model, we can use a unitary rotation to map  $\sigma_x$  to  $\sigma_z$ . This is achieved by

$$\mathcal{H}' = e^{i\pi/4\sigma_y} \mathcal{H} e^{-i\pi/4\sigma_y} = \frac{1}{2} \begin{pmatrix} 1 & 1 \\ -1 & 1 \end{pmatrix} \mathcal{H} \begin{pmatrix} 1 & -1 \\ 1 & 1 \end{pmatrix}. \quad (2.2)$$

	Kitaev	SSH	Kitaev MF
PHS (+1)	$\sigma_x \mathcal{H}^* \sigma_x = -\mathcal{H}$	$\sigma_z H_{\text{SSH}}^* \sigma_z = -H_{\text{SSH}}$	$\mathcal{A}^* = \mathcal{A}$
TRS (+1)	$\mathcal{H}^* = \mathcal{H}$	$H_{\text{SSH}}^* = H_{\text{SSH}}$	$\sigma_z \mathcal{A}^* \sigma_z = -\mathcal{A}$
CS	$\sigma_x \mathcal{H} \sigma_x = -\mathcal{H}$	$\sigma_z H_{\text{SSH}} \sigma_z = -H_{\text{SSH}}$	$\sigma_z \mathcal{A} \sigma_z = -\mathcal{A}$

Table 2.1: The symmetries of the Kitaev wire and the Su–Schrieffer–Heeger (SSH) model. In the last column, the representation of the symmetries on the real matrix  $\mathcal{A}$  representing the Kitaev wire with Majorana Fermions.

Substituting Eq. (1.21), this corresponds to

$$\mathcal{H}' = \begin{pmatrix} i(\text{Im } h + \text{Im } \Delta) & -\text{Re } h + \text{Re } \Delta \\ -\text{Re } h - \text{Re } \Delta & i(\text{Im } h - \text{Im } \Delta) \end{pmatrix}. \quad (2.3)$$

This is a Hermitian matrix because  $h$  is Hermitian and  $\Delta$  is antisymmetric. The symmetries of  $\mathcal{H}'$  are represented by the same operators as those of the SSH model.

### 2.1.2 This corresponds to the introduction of Majorana fermions

On the level of the fermion operators, the basis transformation above corresponds to

$$\hat{H} - \frac{1}{2} \text{Tr} h = \frac{1}{8} \begin{pmatrix} \hat{\mathbf{c}}^\dagger & \hat{\mathbf{c}} \end{pmatrix} \begin{pmatrix} 1 & -1 \\ 1 & 1 \end{pmatrix} \begin{pmatrix} 1 & 1 \\ -1 & 1 \end{pmatrix} \mathcal{H} \begin{pmatrix} 1 & -1 \\ 1 & 1 \end{pmatrix} \begin{pmatrix} 1 & 1 \\ -1 & 1 \end{pmatrix} \begin{pmatrix} \hat{\mathbf{c}} \\ \hat{\mathbf{c}}^\dagger \end{pmatrix} \quad (2.4)$$

$$= \frac{1}{8} \begin{pmatrix} \hat{\mathbf{b}} & i\hat{\mathbf{a}} \end{pmatrix} \mathcal{H}' \begin{pmatrix} \hat{\mathbf{b}} \\ -i\hat{\mathbf{a}} \end{pmatrix}, \quad (2.5)$$

where we introduced Majorana fermions according to

$$\hat{b}_j = \hat{c}_j + \hat{c}_j^\dagger; \quad (2.6a)$$

$$\hat{a}_j = -i(\hat{c}_j - \hat{c}_j^\dagger). \quad (2.6b)$$

These so-called Majorana fermions are often used to treat superconducting systems. They are self-adjoint fermionic operators, so that for any  $j, l$ :

$$\hat{a}_j^\dagger = \hat{a}_j; \quad \hat{b}_j^\dagger = \hat{b}_j; \quad (2.7)$$

$$\{\hat{a}_j, \hat{b}_l\} = 0; \quad \{\hat{a}_j, \hat{a}_l\} = \{\hat{b}_j, \hat{b}_l\} = 2\delta_{jl}. \quad (2.8)$$

Inverting these relations show that the self-adjoint Majorana operators are the “real” and “imaginary part” of the operator  $\hat{c}$ ,

$$\hat{c}_j = \hat{b}_j + i\hat{a}_j; \quad \hat{c}_j^\dagger = \hat{b}_j - i\hat{a}_j. \quad (2.9)$$

### 2.1.3 The last basis transformation rewrites the Hamiltonian in terms of Majorana fermions

Since it is PHS that plays a central role, it is worthwhile to make yet another unitary basis transformation that simplifies its representation. We define

$$\mathcal{H}'' = \begin{pmatrix} 1 & 0 \\ 0 & i \end{pmatrix} \mathcal{H}' \begin{pmatrix} 1 & 0 \\ 0 & -i \end{pmatrix} = \frac{1}{2} \begin{pmatrix} 1 & 1 \\ -i & i \end{pmatrix} \mathcal{H} \begin{pmatrix} 1 & i \\ 1 & -i \end{pmatrix}. \quad (2.10)$$

We can investigate what the symmetries of  $\mathcal{H}$  are mapped into. These are the particle-hole symmetry  $\sigma_x K$ , the time-reversal symmetry  $K$ , and the chiral symmetry  $\sigma_x$ , for which we have

$$\frac{1}{2} \begin{pmatrix} 1 & 1 \\ -i & i \end{pmatrix} \sigma_x K \begin{pmatrix} 1 & i \\ 1 & -i \end{pmatrix} = \frac{1}{2} \begin{pmatrix} 1 & 1 \\ -i & i \end{pmatrix} \begin{pmatrix} 1 & i \\ 1 & -i \end{pmatrix} K = K; \quad (2.11)$$

$$\frac{1}{2} \begin{pmatrix} 1 & 1 \\ -i & i \end{pmatrix} K \begin{pmatrix} 1 & i \\ 1 & -i \end{pmatrix} = \frac{1}{2} \begin{pmatrix} 1 & 1 \\ -i & i \end{pmatrix} \begin{pmatrix} 1 & -i \\ 1 & i \end{pmatrix} K = \sigma_z K; \quad (2.12)$$

$$\frac{1}{2} \begin{pmatrix} 1 & 1 \\ -i & i \end{pmatrix} \sigma_x \begin{pmatrix} 1 & i \\ 1 & -i \end{pmatrix} = \frac{1}{2} \begin{pmatrix} 1 & 1 \\ -i & i \end{pmatrix} \begin{pmatrix} 1 & -i \\ 1 & i \end{pmatrix} = \sigma_z. \quad (2.13)$$

These results are also included in Table 2.1.

In other words,  $\mathcal{H}''$  is a Hermitian matrix with all elements purely imaginary. Thus it can be written as  $i$  times a real antisymmetric matrix,

$$\mathcal{H}'' = i\mathcal{A}; \quad A_{mn} \in \mathbb{R} \quad \text{for } m, n = 1, \dots, 2n; \quad (2.14)$$

$$\mathcal{A} = -i \begin{pmatrix} 1 & 1 \\ -i & i \end{pmatrix} \mathcal{H} \begin{pmatrix} 1 & i \\ 1 & -i \end{pmatrix} = \begin{pmatrix} \text{Im } h + \text{Im } \Delta & \text{Re } h - \text{Re } \Delta \\ -\text{Re } h - \text{Re } \Delta & \text{Im } h - \text{Im } \Delta \end{pmatrix}. \quad (2.15)$$

On the level of the Fock-space Hamiltonian, this corresponds to rewriting it in terms of the Majorana fermions,

$$\hat{H} - \frac{1}{2} \text{Tr} h = \frac{i}{8} \begin{pmatrix} \hat{\mathbf{b}} & \hat{\mathbf{a}} \end{pmatrix} \mathcal{A} \begin{pmatrix} \hat{\mathbf{b}} \\ \hat{\mathbf{a}} \end{pmatrix}. \quad (2.16)$$

#### Time-reversal and chiral symmetries

If the matrix elements of  $\mathcal{H}$  are all real, we also have time-reversal symmetry. This translates to reality of matrix elements of  $\mathcal{H}'$ , and thus,

$$\sigma_z \mathcal{H}''^* \sigma_z = \mathcal{H}''; \quad (2.17)$$

$$\sigma_z \mathcal{A}^* \sigma_z = -\mathcal{A}. \quad (2.18)$$

In the time-reversal symmetric case, get chiral symmetry for free, which is represented on  $\mathcal{H}''$  in the same way as in the SSH model,

$$\sigma_z \mathcal{H}'' \sigma_z = -\mathcal{H}''; \quad (2.19)$$

$$\sigma_z \mathcal{A} \sigma_z = -\mathcal{A}. \quad (2.20)$$

### 2.1.4 The Kitaev wire is more robust than the SSH model

The topological protection of the edge states in the SSH model depended on two fragile features: the robustness of the chiral symmetry and the indivisibility of the unit cell. An isolated edge state can be moved away from 0 energy by breaking chiral symmetry. This is easily realized, e.g., using an onsite potential. On the other hand, just changing the chain termination by adding an extra site is enough to move a bound state from 0 energy as well.

In the Kitaev wire, both the particle-hole symmetry and the indivisibility of the unit cell are hardwired into the formalism, and therefore are robust. Thus Majorana fermions as end states are more robust.

## 2.2 Majorana fermion operators have simple properties

Given a set  $\underline{\hat{\gamma}}$  of Majorana fermions,

$$\underline{\hat{\gamma}} = \{\hat{\gamma}_1, \hat{\gamma}_2, \dots, \hat{\gamma}_{2n}\} = a_1, b_1, a_2, b_2, \dots, a_n, b_n, \quad (2.21)$$

we consider some of their properties.

### 2.2.1 Majorana fermions transform well under real orthogonal transformations

If we mix Majorana fermion operators using a real orthogonal transformation,

$$\underline{\hat{\eta}} = \underline{\mathcal{O}} \underline{\hat{\gamma}}, \quad (2.22)$$

the new operators  $\hat{\eta}_j$  are also Majorana fermions.

This property is useful later when we use the Pfaffian.

### 2.2.2 For complex pair potential, there is a more practical way to introduce Majorana fermions

We can generalize the formulas for the Majorana fermions. We can use

$$\hat{b}_j = e^{-i\phi_j/2} \hat{c}_j + e^{i\phi_j/2} \hat{c}_j^\dagger; \quad (2.23a)$$

$$\hat{a}_j = -i \left( e^{-i\phi_j/2} \hat{c}_j - e^{i\phi_j/2} \hat{c}_j^\dagger \right). \quad (2.23b)$$

These relations can be inverted to give

$$\hat{c}_j = \frac{e^{i\phi_j/2}}{2} (\hat{b}_j + i\hat{a}_j); \quad (2.24a)$$

$$\hat{c}_j^\dagger = \frac{e^{-i\phi_j/2}}{2} (\hat{b}_j - i\hat{a}_j). \quad (2.24b)$$

The Hermitian (“real”) Majorana fermion operators are the “real parts” and “imaginary parts” of the original (“complex”) fermion operators  $\hat{c}$ . There is a free parameter  $\phi_j$ , which we can set to the phase of the  $p$ -wave order parameter:  $\Delta_j = \Delta_j e^{i\phi_j}$ , with  $\Delta_j$  denoting its absolute value.

Rewriting the Hamiltonian in terms of the Majorana operators introduced in Eq. (2.23) above, corresponds to a transformation on the Bogoliubov-de Gennes Hamiltonian. Starting from Eq. (1.21), we have:

## 2.3 Pfaffian and the ground-state parity

The fermion parity of the ground state is a topological invariant of a 0-dimensional superconductor. In the noninteracting case it can be directly computed from the Bogoliubov-de Gennes Hamiltonian using the Pfaffian.

### 2.3.1 Pfaffian

In this section we review the Pfaffian, an important tool for skew symmetric matrices.

We consider an  $M \times M$  skew symmetric matrix  $A$ , with matrix elements  $a_{lm}$ , i.e.,

$$A^T = -A; \quad a_{lm} = -a_{ml}. \quad (2.25)$$

The determinant of such a matrix is a homogeneous  $M$ th order polynomial of its matrix elements.

If the matrix is odd dimensional,  $M = 2N + 1$ , its determinant vanishes;

$$M = 2N + 1 : \quad \det A = \det A^T = \det(-A) = (-1)^{2N+1} \det A = -\det A. \quad (2.26)$$

If, on the other hand, the matrix is even dimensional, the determinant can be written as the complete square of a homogeneous  $M/2$ th order polynomial of the matrix elements. This polynomial is known as the Pfaffian.

$$M = 2N : \quad \det A = (\text{Pf}A)^2. \quad (2.27)$$

Its definition and further properties follow below.

#### The Pfaffian is a homogeneous polynomial of the matrix elements

The polynomial is defined in the following way. Consider the partitions of the indices  $\{1, 2, \dots, 2N\}$  into pairs, without regard to order,

$$\alpha = \{(j_1, m_1), (j_2, m_2), \dots, (j_n, m_n)\}, \quad (2.28)$$

with  $j_n < m_n$  for every  $n = 1, \dots, N$ , and  $j_1 < j_2 < \dots < j_N$ . We can regard each partition as a permutation,

$$\pi_\alpha = \begin{bmatrix} 1 & 2 & 3 & 4 & \cdots & 2n-1 & 2n \\ i_1 & j_1 & i_2 & j_2 & \cdots & i_n & j_n \end{bmatrix}. \quad (2.29)$$

The Pfaffian is

$$\text{Pf}(A) = \sum_{\alpha \in \Pi} \text{sgn}(\pi_\alpha) a_{i_1, j_1} a_{i_2, j_2} \cdots a_{i_n, j_n}. \quad (2.30)$$

### Important properties

We list some important properties of the Pfaffian, which are easy to prove or are detailed in the notes by Haber.

For a block-diagonal matrix, we have

$$A_1 \oplus A_2 = \begin{bmatrix} A_1 & 0 \\ 0 & A_2 \end{bmatrix}; \quad (2.31)$$

$$\text{Pf}(A_1 \oplus A_2) = \text{Pf}(A_1)\text{Pf}(A_2). \quad (2.32)$$

For an arbitrary  $2N \times 2N$  matrix  $B$ ,

$$\text{Pf}(BAB^T) = \det(B)\text{Pf}(A). \quad (2.33)$$

### The Pfaffian is related to the normal form

The Householder transformations are normally used to bring a real symmetric matrix to a tridiagonal form. They are conjugations by suitably chosen orthogonal matrices  $P_j$ , each has determinant  $-1$ . See the note attached.

Take a real and skew-symmetric matrix  $A$ .

$$P_{2N} \dots P_2 P_1 A P_1 P_2 \dots P_{2N} = A_{\text{tri}}, \quad (2.34)$$

where

$$A_{\text{tri}} = \begin{pmatrix} 0 & \lambda_1 & 0 & 0 & \dots & 0 \\ -\lambda_1 & 0 & \lambda_2 & 0 & \dots & 0 \\ 0 & -\lambda_2 & 0 & \ddots & \dots & \vdots \\ & & \ddots & 0 & \ddots & \\ 0 & & & \ddots & 0 & \lambda_{N-1} \\ \vdots & \vdots & & & -\lambda_{N-1} & 0 \end{pmatrix} \quad (2.35)$$

It can easily be shown that the Pfaffian of such a matrix is the product of half of the  $\lambda$ ,

$$\text{Pf}(A_{\text{tri}}) = \lambda_1 \lambda_3 \dots \lambda_{N-1}. \quad (2.36)$$

Using the property in Eq. (2.33) above,

$$\text{Pf}(A) = \det(P_1) \det(P_2) \dots \det(P_{2N}) \text{Pf}(A_{\text{tri}}) = \lambda_1 \lambda_3 \dots \lambda_{N-1}. \quad (2.37)$$

## 2.4 Pfaffian of the Bogoliubov-de Gennes Hamiltonian is the ground state parity

### 2.5 Exercises

Express the Hamiltonian in the Majorana basis. Show that in the simple cases a)  $\Delta = t = 0$  and b)  $\mu = 0$ ,  $\Delta = \pm\mu$  the Hamiltonian can be diagonalized easily. What are the independent fermionic operators  $d$ ?



## Chapter 3

# Two Majorana Fermions can be used to hide a qubit

The Kitaev wire has separated Majorana fermions localized at the left and the right end. We can use these to hide quantum information.

### 3.1 The eigenmodes of the flat-band limit Kitaev wire

In the nontrivial flat-band limit the Kitaev wire is simple to solve. We set  $\Delta = t = 1$  and  $\mu = 0$  in the Hamiltonian, which for a wire of  $N$  sites reads

$$\hat{H}_K = \sum_{j=1}^{N-1} \left( \hat{c}_j^\dagger \hat{c}_{j+1} + \hat{c}_j \hat{c}_{j+1} + h.c. \right) \quad (3.1)$$

We can rewrite this using the Majorana fermions of Eq. (2.6),

$$\hat{H}_K = \sum_j \left( \hat{c}_j^\dagger + \hat{c}_j \right) \left( \hat{c}_{j+1} - \hat{c}_{j+1}^\dagger \right) = \sum_{j=1}^{N-1} i \hat{b}_j \hat{a}_{j+1}. \quad (3.2)$$

The eigenmodes  $\hat{d}_j$  of the Hamiltonian are identified as

$$\hat{d}_j = \frac{\hat{b}_j + i \hat{a}_{j+1}}{2} = \frac{\hat{c}_j + \hat{c}_j^\dagger + \hat{c}_{j+1} - \hat{c}_{j+1}^\dagger}{2}; \quad (3.3)$$

$$\hat{d}_j^\dagger = \frac{\hat{b}_j - i \hat{a}_{j+1}}{2} = \frac{\hat{c}_j + \hat{c}_j^\dagger - \hat{c}_{j+1} + \hat{c}_{j+1}^\dagger}{2}, \quad (3.4)$$

since

$$2 \hat{d}_j^\dagger \hat{d}_j - 1 = \frac{1}{2} \left( \hat{b}_j - i \hat{a}_{j+1} \right) \left( \hat{b}_j + i \hat{a}_{j+1} \right) - 1 = i \hat{b}_j \hat{a}_{j+1}. \quad (3.5)$$

We also introduce a complex fermion operator composed of the edge Majorana fermions,

$$\hat{d} = \frac{\hat{b}_N + i\hat{a}_1}{2} = \frac{\hat{c}_N + \hat{c}_N^\dagger + \hat{c}_1 - \hat{c}_1^\dagger}{2}. \quad (3.6)$$

This is a fermion that is split equally between the two ends. Using these, the Kitaev wire Hamiltonian reads

$$\hat{H}_K = 2 \sum_{j=1}^{N-1} \hat{d}_j^\dagger \hat{d}_j - (N-1). \quad (3.7)$$

## 3.2 The ground state is an equal superposition of all Fock states of fixed parity

### 3.2.1 Computational basis notation

We define a computational basis notation as below:

$$|000\rangle = |\emptyset\rangle; \quad (3.8)$$

$$|100\rangle = \hat{c}_1^\dagger |\emptyset\rangle; \quad (3.9)$$

$$|101\rangle = \hat{c}_3^\dagger \hat{c}_1^\dagger |\emptyset\rangle. \quad (3.10)$$

Note that the order of the operators is important.

$$\hat{c}_3 |101\rangle = |100\rangle; \quad (3.11)$$

$$\hat{c}_1 |101\rangle = -|001\rangle. \quad (3.12)$$

We also introduce a shorthand for bit sequences. We let  $\underline{\alpha}$  denote a sequence of 1's and 0's, and  $|\underline{\alpha}|$  is the number of 1's in the sequence. E.g.

$$\underline{\alpha} = (0, 1, 0, 1, 1); \quad |\underline{\alpha}\rangle = |0, 1, 0, 1, 1\rangle; \quad |\underline{\alpha}| = 3. \quad (3.13)$$

### 3.2.2 Statement

The even and odd ground states of the Kitaev wire are equal superpositions of all allowed computational basis states,

$$|e\rangle = 2^{\frac{1-N}{2}} \sum_{\alpha: |\underline{\alpha}| \text{ even}} (-1)^{P_\alpha} |\underline{\alpha}\rangle; \quad |o\rangle = 2^{\frac{1-N}{2}} \sum_{\alpha: |\underline{\alpha}| \text{ odd}} (-1)^{P_\alpha} |\underline{\alpha}\rangle. \quad (3.14)$$

Here  $P_\alpha$  is the parity of the number steps necessary to reach the sequence  $\alpha$  from a reference sequence. A step is a simultaneous flip of two neighboring bits. This can result in a) adding two fermions, b) deleting two fermions, or c) moving a fermion. The reference sequence can be chosen as  $(0, 0, \dots, 0)$  for the even state, and  $(1, 0, \dots, 0)$  for the odd state.

E.g., for  $N = 2$ ,

$$|e\rangle = \frac{|00\rangle - |11\rangle}{\sqrt{2}}; \quad |o\rangle = \frac{|01\rangle - |10\rangle}{\sqrt{2}}; \quad (3.15)$$

for  $N = 3$ , we have

$$|e\rangle = \frac{|000\rangle - |011\rangle + |101\rangle - |110\rangle}{2}; \quad (3.16)$$

$$|o\rangle = \frac{|001\rangle - |010\rangle + |100\rangle - |111\rangle}{2}. \quad (3.17)$$

### 3.2.3 Proof

The Ground State  $|GS\rangle$  is a superposition of basis states that is annihilated by all the eigenmode operators  $\hat{d}_j$ . We fix a value of  $m$ , focus on the requirement

$$\hat{d}_j |GS\rangle = (\hat{c}_j + \hat{c}_j^\dagger + \hat{c}_{j+1} - \hat{c}_{j+1}^\dagger) |GS\rangle = 0. \quad (3.18)$$

We can write the Ground State as

$$|GS\rangle = \sum_{\underline{\alpha}, \underline{\beta}} a_{\underline{\alpha}, \underline{\beta}} |\underline{\beta} 0 0 \underline{\alpha}\rangle + b_{\underline{\alpha}, \underline{\beta}} |\underline{\beta} 0 1 \underline{\alpha}\rangle + c_{\underline{\alpha}, \underline{\beta}} |\underline{\beta} 1 0 \underline{\alpha}\rangle + d_{\underline{\alpha}, \underline{\beta}} |\underline{\beta} 1 1 \underline{\alpha}\rangle. \quad (3.19)$$

For one term in the above sum, Eq. (3.18) can be written using a compact vector notation as

$$\begin{pmatrix} a \\ b \\ c \\ d \end{pmatrix} \xrightarrow{\hat{d}_j} (-1)^{|\underline{\alpha}|} \left\{ \begin{pmatrix} c \\ -d \\ 0 \\ 0 \end{pmatrix} + \begin{pmatrix} 0 \\ 0 \\ a \\ -b \end{pmatrix} + \begin{pmatrix} b \\ 0 \\ d \\ 0 \end{pmatrix} - \begin{pmatrix} 0 \\ a \\ 0 \\ c \end{pmatrix} \right\} = \begin{pmatrix} 0 \\ 0 \\ 0 \\ 0 \end{pmatrix}. \quad (3.20)$$

Independent of whether  $|\underline{\alpha}|$  is odd or even, this can be summarized in two equations,

$$a_{\underline{\alpha}, \underline{\beta}} = -d_{\underline{\alpha}, \underline{\beta}}; \quad b_{\underline{\alpha}, \underline{\beta}} = -c_{\underline{\alpha}, \underline{\beta}}. \quad (3.21)$$

Therefore, for any sequence  $\underline{\alpha}$ , whenever two neighbouring bits in the sequence are flipped, the corresponding amplitudes must have opposite signs.

### 3.2.4 The ground state of the closed wire is odd/even if the number of sites is even/odd

For the sake of completeness, consider a closed Kitaev wire in the flat band limit. The Hamiltonian reads

$$\begin{aligned} \hat{H}_K &= \sum_{j=1}^{N-1} (\hat{c}_j^\dagger \hat{c}_{j+1} + \hat{c}_j \hat{c}_{j+1} + h.c.) + (\hat{c}_N^\dagger \hat{c}_1 + \hat{c}_N \hat{c}_1 + h.c.) \\ &= \sum_{j=1}^{N-1} i\hat{b}_j \hat{a}_{j+1} + i\varepsilon \hat{b}_N \hat{a}_1 = 2 \sum_{j=1}^{N-1} \hat{d}_j^\dagger \hat{d}_j + 2\hat{d}^\dagger \hat{d} - N. \end{aligned} \quad (3.22)$$

We now have an extra condition on the ground state: the edge fermion operator  $\hat{d}$  has to annihilate it. As in the previous Section, we take

$$|GS\rangle = \sum_{\underline{\alpha}} a_{\underline{\alpha}} |0 \underline{\alpha} 0\rangle + b_{\underline{\alpha}} |1 \underline{\alpha} 0\rangle + c_{\underline{\alpha}} |0 \underline{\alpha} 1\rangle + d_{\underline{\alpha}} |1 \underline{\alpha} 1\rangle. \quad (3.23)$$

The extra requirement is

$$\left( \hat{c}_N + \hat{c}_N^\dagger + \hat{c}_1 - \hat{c}_1^\dagger \right) |GS\rangle = 0, \quad (3.24)$$

which has to hold also for all  $\underline{\alpha}$  separately. This gives

$$\begin{pmatrix} a \\ b \\ c \\ d \end{pmatrix} \xrightarrow{\hat{d}} \begin{pmatrix} c \\ d \\ 0 \\ 0 \end{pmatrix} + \begin{pmatrix} 0 \\ 0 \\ a \\ b \end{pmatrix} + (-1)^{|\underline{\alpha}|} \left\{ \begin{pmatrix} b \\ 0 \\ -d \\ 0 \end{pmatrix} - \begin{pmatrix} 0 \\ a \\ 0 \\ -c \end{pmatrix} \right\} = \begin{pmatrix} 0 \\ 0 \\ 0 \\ 0 \end{pmatrix}. \quad (3.25)$$

This can be summarized in two equations,

$$a_{\underline{\alpha}} = (-1)^{|\underline{\alpha}|} d_{\underline{\alpha}}; \quad b_{\underline{\alpha}} = -(-1)^{|\underline{\alpha}|} c_{\underline{\alpha}}. \quad (3.26)$$

However,  $(1\underline{\alpha}1)$  can be reached from  $(0\underline{\alpha}0)$  in  $N - 1$  steps, and therefore,

$$a_{\underline{\alpha}} = (-1)^{N-1} d_{\underline{\alpha}}; \quad b_{\underline{\alpha}} = (-1)^{N-1} c_{\underline{\alpha}}. \quad (3.27)$$

Comparing these sets of equations tells us that if  $N$  is even, for  $a_{\underline{\alpha}}$  and  $d_{\underline{\alpha}}$  we must have an odd number of fermions in  $\underline{\alpha}$ , but for  $b_{\underline{\alpha}}$  and  $c_{\underline{\alpha}}$ , an even number of fermions in  $\underline{\alpha}$ . Altogether then, for  $N$  even, the total number of fermions must be odd. The same logic applies to  $N$  odd, and we obtain

$$\text{closed Kitaev wire, } N \text{ even : } |GS\rangle = |o\rangle; \quad |e\rangle = \hat{d}^\dagger |o\rangle; \quad (3.28a)$$

$$\text{closed Kitaev wire, } N \text{ odd : } |GS\rangle = |e\rangle; \quad |o\rangle = \hat{d}^\dagger |e\rangle. \quad (3.28b)$$

### 3.3 Tunneling between a dot and a wire

The even and odd ground states of the Kitaev wire can be used to form a protected qubit. These two states form a degenerate subspace, where no quantum operations happen: transitions are forbidden because parity is conserved, and degeneracy is protected by the gap and the superconductivity.

We will use the edge fermion  $\hat{d}$  to define the qubit, and so introduce the ground state without/with this fermion as

$$\forall j : \hat{d}_j |GS_0\rangle = 0; \quad \hat{d} |GS_0\rangle = 0; \quad \hat{d}^\dagger |GS_0\rangle = |GS_1\rangle; \quad (3.29a)$$

$$\forall j : \hat{d}_j |GS_1\rangle = 0; \quad \hat{d} |GS_1\rangle = |GS_0\rangle; \quad \hat{d}^\dagger |GS_1\rangle = 0. \quad (3.29b)$$

In light of Eqs. (3.28), we have

$$N \text{ even : } |GS_0\rangle = |o\rangle; \quad N \text{ odd : } |GS_0\rangle = |e\rangle. \quad (3.30a)$$

A qubit in this basis is

$$|\Psi_{MF}\rangle = \alpha |GS_0\rangle + \beta |GS_1\rangle; \quad \alpha, \beta \in \mathbb{C}; \quad |\alpha|^2 + |\beta|^2 = 1. \quad (3.31)$$

We now try to write and read this memory by connecting it through a tunnel barrier with an unprotected qubit, an electron on a quantum dot. We assume that the dot has been initialized in a qubit state,

$$|\Psi_D(t=0)\rangle = \alpha |0\rangle + \beta |1\rangle; \quad \alpha, \beta \in \mathbb{C}; \quad |\alpha|^2 + |\beta|^2 = 1. \quad (3.32)$$

We will connect the Kitaev wire to the dot through some perturbation  $\gamma \hat{H}_1$ , wait for some time  $t$ , disconnect the two systems. In the final state, we would like to see the qubit transcribed from the dot to the wire, i.e.,

$$|\Psi(t=0)\rangle = \alpha |0_D, GS_0\rangle + \beta |1_D, GS_0\rangle; \quad (3.33)$$

$$|\Psi(t)\rangle = \alpha |0_D, GS_0\rangle + \beta |0_D, GS_1\rangle. \quad (3.34)$$

### 3.3.1 Projecting the dynamics to the low energy subspace

All the schemes for qubit transcription we detail below will work in the tunneling limit, and we will use quasi-degenerate perturbation theory to describe them. We will find it enough to go to first order in the small parameter  $\gamma$ . This means that we will

1. identify the low-energy subspace,
2. project the full Hamiltonian onto this subspace.

### 3.3.2 Bending a wire to address the edge fermion

The first idea is to access the protected qubit directly, i.e., address the edge fermion operator  $\hat{d}$ , by coupling the quantum dot to both ends. This can be achieved by bending the Kitaev wire into a U shape. The Hamiltonian reads

$$\hat{H}_{d2} = \hat{H}_K + \gamma \left( \underbrace{\hat{c}_0^\dagger (\hat{c}_1 + \hat{c}_N) + h.c.}_{\hat{H}_1} \right). \quad (3.35)$$

The low energy subspace is spanned by the states  $\{|0\rangle_D |GS_0\rangle, |0\rangle_D |GS_1\rangle, |1\rangle_D |GS_0\rangle, |1\rangle_D |GS_1\rangle\}$ . We can find the projected Hamiltonian by rewriting the annihilation operator  $\hat{c}_1$  in terms of the eigenmodes of  $\hat{H}_K$ , as

$$\hat{c}_1 = \frac{1}{2} (\hat{b}_1 + i\hat{a}_1) = \frac{1}{2} (\hat{d}_1 + \hat{d}_1^\dagger + \hat{d} - \hat{d}^\dagger); \quad (3.36a)$$

$$\hat{c}_N = \frac{1}{2} (\hat{b}_N + i\hat{a}_N) = \frac{1}{2} (\hat{d} + \hat{d}^\dagger + \hat{d}_{N-1} - \hat{d}_{N-1}^\dagger). \quad (3.36b)$$

Each of the operators  $\hat{d}_j$  and  $\hat{d}_j^\dagger$  take us outside the low energy subspace (by annihilating a state or by creating a nonzero-energy excitation). Projection to the low energy subspace is thus achieved by

$$\hat{c}_1 \rightarrow \frac{i}{2}\hat{a}_1 = \frac{1}{2}(\hat{d} - \hat{d}^\dagger); \quad (3.37a)$$

$$\hat{c}_N \rightarrow \frac{1}{2}\hat{b}_N = \frac{1}{2}(\hat{d} + \hat{d}^\dagger). \quad (3.37b)$$

We obtain the projected version of the Hamiltonian as

$$\hat{H}_{d2} = \gamma\hat{c}_0^\dagger\hat{d} + h.c. \quad (3.38)$$

The low energy subspace falls apart to two subspaces of different parity. These are defined by the projectors,

$$\hat{P}_0 = |0_D, GS_0\rangle\langle 0_D, GS_0| + |1_D, GS_1\rangle\langle 1_D, GS_1|; \quad (3.39)$$

$$\hat{P}_1 = |1_D, GS_0\rangle\langle 1_D, GS_0| + |0_D, GS_1\rangle\langle 0_D, GS_1|. \quad (3.40)$$

Projecting the Hamiltonian  $\hat{H}_{d2}$ , to these subspaces gives

$$\hat{H}_{d2,0} = 0; \quad \hat{H}_{d2,1} = \gamma\sigma_x. \quad (3.41)$$

Therefore, in the low energy subspace given by  $\hat{P}_0$  there is no dynamics, while in subspace  $\hat{P}_1$ , we have  $\cos(\gamma t) - \sin(\gamma t)\sigma_x$ . This describes a single electron performing Rabi oscillations between the dot and the wire.

We can now identify the low energy dynamics, started from the state

$$|\Psi(t=0)\rangle = \alpha|0_D, GS_0\rangle + \beta|1_D, GS_0\rangle. \quad (3.42)$$

We find

$$|\Psi(t)\rangle = \alpha|0_D, GS_0\rangle + \beta(\cos(\gamma t)|1_D, GS_0\rangle - i\sin(\gamma t)|0_D, GS_1\rangle) \quad (3.43)$$

Thus, setting the time right ( $\pi$ -pulse of  $\gamma$ ), we have

$$|\Psi(t = (2n+1)\pi/(2\gamma))\rangle = \alpha|0_D, GS_0\rangle - i\beta|0_D, GS_1\rangle. \quad (3.44)$$

We find that we successfully transcribed the qubit from the dot to the wire, up to a unitary transformation  $e^{-i\pi/2(\sigma_z - \sigma_0)}$ . This can be included by defining the qubit basis as

$$|0\rangle = |GS_0\rangle; \quad |1\rangle = -i|GS_1\rangle. \quad (3.45)$$

### Readout is simple

The Rabi oscillation of a single electron between the dot and the wire can also be used to read out the wire qubit. Take as initial state

$$|\Psi(t=0)\rangle = \alpha|0_D, GS_0\rangle + \beta|0_D, GS_1\rangle. \quad (3.46)$$

We find

$$|\Psi(t)\rangle = \alpha |0_D, GS_0\rangle + \beta (\cos(\gamma t) |0_D, GS_1\rangle - i \sin(\gamma t) |1_D, GS_0\rangle). \quad (3.47)$$

Thus, setting the time right ( $\pi$ -pulse of  $\gamma$ ), we have

$$|\Psi(t = (2n + 1)\pi/(2\gamma))\rangle = \alpha |0_D, GS_0\rangle - i\beta |1_D, GS_0\rangle. \quad (3.48)$$

We find that we successfully transcribed the qubit from the wire to the dot, up to a unitary transformation  $e^{-i\pi/2(\sigma_z - \sigma_0)}$ .

### The couplings to the two ends have to be equal

If the dot is not coupled symmetrically to the first and the last site, we have a problem. The Hamiltonian reads

$$\hat{H}_{d2} = \hat{H}_K + \gamma_L (\hat{c}_0^\dagger \hat{c}_1 + \hat{c}_1^\dagger \hat{c}_0) + \gamma_R (\hat{c}_0^\dagger \hat{c}_N + \hat{c}_N^\dagger \hat{c}_0). \quad (3.49)$$

In the low energy subspace, this is ...

### 3.3.3 Coupling to the wire from one end

It might be simpler to couple a dot to one end of a Kitaev wire only, rather than both ends with the same coupling amplitudes. The Hamiltonian reads

$$\hat{H}_{d1} = \hat{H}_K + \gamma (\hat{c}_0^\dagger \hat{c}_1 + \hat{c}_1^\dagger \hat{c}_0). \quad (3.50)$$

The projected Hamiltonian, obtained using Eqs. (3.37), reads

$$\hat{H}_{d1} = \frac{\gamma}{2} \hat{c}_0^\dagger (\hat{d} - \hat{d}^\dagger) + h.c. \quad (3.51)$$

We now have nontrivial Hamiltonians in both the even and the odd parity subspaces,

$$\hat{H}_{d1,0} = -\frac{\gamma}{2} \sigma_x; \quad \hat{H}_{d1,1} = \frac{\gamma}{2} \sigma_x. \quad (3.52)$$

The time evolution reveals simultaneous Rabi oscillations in the two subspaces. Started from the state

$$|\Psi(t = 0)\rangle = \alpha |0_D, GS_0\rangle + \beta |1_D, GS_0\rangle, \quad (3.53)$$

we find

$$\begin{aligned} |\Psi(t)\rangle &= \alpha (\cos(\gamma t) |0_D, GS_0\rangle + i \sin(\gamma t) |1_D, GS_1\rangle) \\ &+ \beta (\cos(\gamma t) |1_D, GS_0\rangle - i \sin(\gamma t) |0_D, GS_1\rangle). \end{aligned} \quad (3.54)$$

Thus, for a  $\pi$ -pulse of  $\gamma$ , we obtain

$$|\Psi(t = (2n + 1)\pi/(2\gamma))\rangle = \alpha |1_D, GS_1\rangle - i\beta |0_D, GS_1\rangle. \quad (3.55)$$

Thus, instead of transferring the quantum state from the dot to the wire, all we achieved was a bit-flip operation on both the dot and the wire.

### An extra measurement can save this scheme

We can still save this scheme if we incorporate an extra measurement of the state of the quantum dot. We first time evolve until time  $t$ , when we have an entangled state. The outcome of the measurement gives 0 or 1, and it acts as a projection of the state. The post-measurement state reads

$$|\Psi(t) : 0\rangle = \alpha \cos(\gamma t) |GS_0\rangle + -i\beta \sin(\gamma t) |GS_1\rangle; \quad (3.56a)$$

$$|\Psi(t) : 1\rangle = \alpha i \sin(\gamma t) |GS_1\rangle + \beta \cos(\gamma t) |GS_0\rangle, \quad (3.56b)$$

where the norm of each of these conditional states is equal to the probability of the corresponding measurement outcome, e.g.,  $\langle \Psi(t) : 0 | \Psi(t) : 0 \rangle = P(0)$ .

For most values of  $t$ , the post-measurement states are not unitary transforms of the initial state. This can be checked by taking the map and multiplying it by the Hermitian conjugate map. This will result in both cases by factors  $\cos^2 \gamma t$  and  $\sin^2 \gamma t$  multiplying  $\alpha$  and  $\beta$  respectively, which is, when normalized back, not equal to unity.

A way to solve this problem is to take a  $\pi/2$ -pulse of  $\gamma$ , i.e.,

$$|\Psi(t = (4n + 1)\pi/(4\gamma)) : 0\rangle = \frac{1}{\sqrt{2}} (\alpha |GS_0\rangle - i\beta |GS_1\rangle); \quad (3.57a)$$

$$|\Psi(t = (4n + 1)\pi/(4\gamma)) : 1\rangle = \frac{1}{\sqrt{2}} (i\alpha |GS_1\rangle + \beta |GS_0\rangle). \quad (3.57b)$$

Here the post-measurement state of the wire is a unitary transform of the original state of the quantum dot.

We can understand the unitary transformation as an error operation, and the measurement on the dot as a diagnosis of the error. Without the measurement result, the quantum information is damaged. Having the measurement result allows us to compensate for the error, e.g., by changing the definition of the basis states.

### No simple way for readout

An important part of the write protocol was the measurement on the quantum dot, the system from which the quantum information was copied. A read protocol would be a transfer of the state of the wire back on the quantum dot. This could work in the same way, if there was a simple way to do a projective measurement on the wire qubit. However, I don't see a simple way.

### 3.3.4 One dot, two wires

## 3.4 Turning the charge-based qubit into a position-based qubit

Two dots, two wires.

### 3.4. TURNING THE CHARGE-BASED QUBIT INTO A POSITION-BASED QUBIT<sup>25</sup>

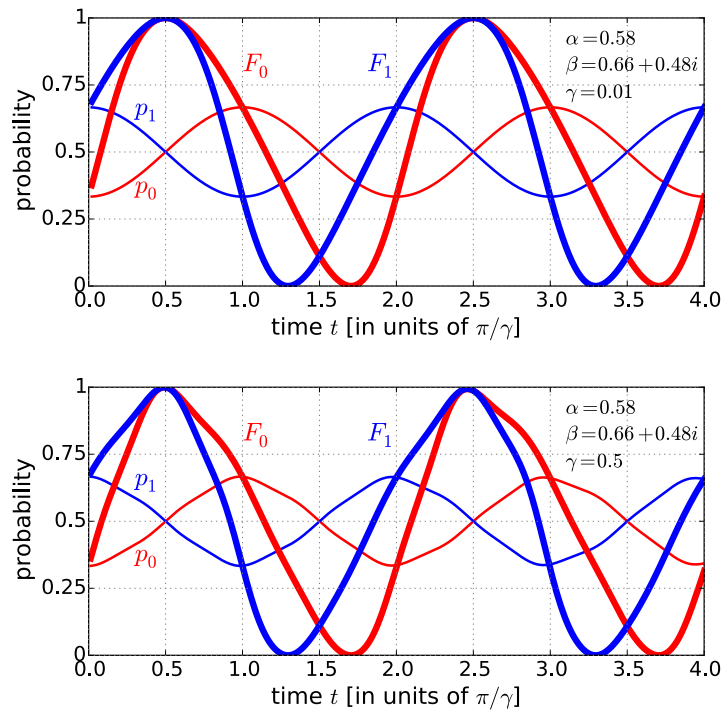


Figure 3.1: Probabilities, fidelities

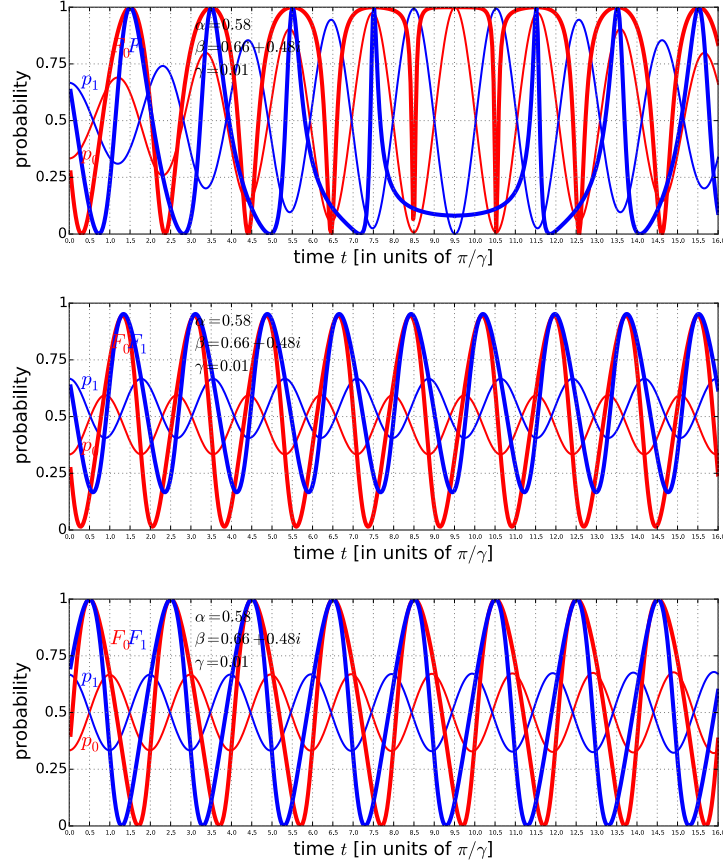


Figure 3.2: Probabilities, fidelities. Kitaev wire with  $t = 1$ ,  $\Delta = 0.9$ .  $N = 3$  (top), 4 (middle) 5 (bottom) sites, plus dot.

### 3.5 The above schemes can all be generalized away from the flat band limit

All we need are Majorana fermion operators.

## 3.6 Exercises

### 3.6.1 Two-site topological Kitaev wire in the dimerized limit

The Hamiltonian:

$$H = c_1^\dagger c_2 + e^{i\varphi} c_1^\dagger c_2^\dagger + h.c. \quad (3.58)$$

Tasks:

1. Write out the matrix of the Fock-space Hamiltonian.
2. Determine the energy eigenstates and eigenvalues. (Even ground state  $|e\rangle$ , odd ground state  $|o\rangle$ , even excited state  $|e'\rangle$ , odd excited state  $|o'\rangle$ )
3. Write out the BdG Hamiltonian.
4. The BdG Hamiltonian describes two independent single-particle fermionic excitations. Determine the BdG wave function of the positive-energy fermionic excitation  $\hat{d}_p^\dagger$ .
5. Determine the zero-energy Majorana eigenvectors of the BdG Hamiltonian that are localized to a given edge of the wire. (Let's call them Majoranas from now on.) Are they unique?
6. Consider the zero-energy fermionic excitation  $\hat{d}_{o\leftarrow e}^\dagger$  that maps  $|e\rangle$  to  $|o\rangle$ . Construct this from the Majoranas. How many ways can you do this?
7. Plot the directed graph showing the relation between the (Fock-space) energy eigenstates and the two independent excitations  $\hat{d}_p^\dagger$  and  $\hat{d}_{o\leftarrow e}^\dagger$ .



# Chapter 4

## Andras

We have seen earlier via two numerical examples, that the qubit formed by the two degenerate ground states of a Kitaev wire can be manipulated by cyclic adiabatic processes. In those processes, the relative Berry phase picked up by the even and odd ground states was either  $\pi/2$  or  $-\pi/2$  or  $\pi$ . Here, we show that these values are generic: as long as the ground states are connected by zero-energy fermionic excitations composed of localized Majorana excitations, braiding of two Majoranas always results in a relative Berry phase of  $n\pi/2$  between the two ground states connected by the two Majoranas.

### 4.1 Preliminary: parallel-transport parametrization

Consider cyclic adiabatic process in a generic quantum system.

Consider the  $n$ th energy eigenstate and assume that it is non-degenerate throughout the whole process. [figure:  $E_n(t)$ ]

The adiabatic time evolution of this state is denoted by  $|n(t)\rangle$ .

Time parametrizations (or gauges) of the instantaneous energy eigenstate are denoted by  $|n_t\rangle$ ,  $t \in [0, T]$ ; these can be cyclic,  $|n_T\rangle = |n_0\rangle$ , or not cyclic,  $|n_T\rangle \neq |n_0\rangle$ .

The parallel-transport time parametrization (PTP) is a non-cyclic one. It is defined via the relation  $\langle n_t | \partial_t | n_t \rangle = 0$ . For a given cyclic-adiabatic process, the parallel-transport parametrization exists and is unique. Moreover, the parallel-transport parametrization is the actual adiabatic time evolution, without the dynamical phase:

$$|n(t)\rangle = e^{-i \int_0^t dt' E_n(t')/\hbar} |n_t\rangle \quad (4.1)$$

We know that the phase factor multiplying the initial state at the end of the process is the product of the dynamical phase factor and the Berry phase

factor:

$$|n(T)\rangle = e^{-i \int_0^T dt' E_n(t')/\hbar} e^{i\gamma_n} |n_0\rangle \quad (4.2)$$

Comparing this with Eq. (4.1) evaluated at  $t = T$ , we find

$$|n_T\rangle = e^{i\gamma_n} |n_0\rangle \quad (4.3)$$

From now on, we disregard dynamical phases, and use  $|n_t\rangle$  and  $|n(t)\rangle$  interchangeably for the dynamics, whenever  $|n_t\rangle$  is a PTP.

The Berry phase factor can be expressed as

$$e^{i\gamma_n} = \langle n_0 | n_T \rangle \quad (4.4)$$

## 4.2 Cyclic adiabatic exchange of the ends of the Kitaev wire

If the two ends of the Kitaev wire are exchanged in a cyclic adiabatic process, then the relative Berry phase of the even and odd ground states will be either  $\pi/2$  or  $-\pi/2$ .

1. Braiding, example: Y-turn in a T-junction [figure]; we have numerically computed that the relative Berry phase between  $|e\rangle$  and  $|o\rangle$  was  $\pi/2$ .
2. *Def: Braiding* is a cyclic adiabatic process under which the two ends of the topological Kitaev wire is exchanged.
3. *Proposition:* Braiding in a long topological Kitaev wire results in a relative Berry phase of  $\pi/2$  or  $-\pi/2$  between the even and odd ground states.
4. Proof of proposition 1, plan: we will evaluate the relative Berry phase factor of the even and odd ground states, that is

$$e^{i\gamma_r} = e^{i(\gamma_o - \gamma_e)} = \langle o_0 | o(T) \rangle \langle e(T) | e_0 | \cdot \rangle \quad (4.5)$$

5. Proof of proposition 1, step 1. Preliminaries.

- (a) (redundant) Disregard dynamical phases for simplicity.
- (b) (redundant) Parametrize the even ground state using the parallel-transport parametrization (PTP). Denote the parametrization as  $|e_t\rangle$ ,  $t \in [0, T]$ . Recall that (i) PTP is not cyclic, (ii) in the PTP, by definition,  $\langle e_t | \partial_t | e_t \rangle = 0$ , (iii) PTP is the same as the adiabatic time evolution without the dynamical phase, (iv) therefore the PTP incorporates the Berry phase, that is,

$$|e(T)\rangle = |e_T\rangle = e^{i\gamma_e} |e_0\rangle. \quad (4.6)$$

- (c) Now we parametrize the zero-energy fermionic excitation  $\hat{d}_{o\leftarrow e}^\dagger$  using the continuous parametrizations of the two edge-localized Majorana operators/eigenvectors  $\hat{\gamma}_{1t} \equiv \psi_{1t} = \begin{pmatrix} \vec{u}_{1t}^* \\ \vec{u}_{1t} \end{pmatrix}$  and  $\hat{\gamma}_{2t} \equiv \psi_{2t} = \begin{pmatrix} \vec{u}_{2t}^* \\ \vec{u}_{2t} \end{pmatrix}$  as

$$\hat{d}_{o\leftarrow e,t}^\dagger := \frac{1}{\sqrt{2}}(\hat{\gamma}_{1t} - i\hat{\gamma}_{2t}). \quad (4.7)$$

- (d) Remark: this parametrization is (almost) unique, unlike the parametrization of a generic finite-energy fermionic excitation with a  $U(1)$  gauge freedom. (almost: there is a sign ambiguity)
- (e) Parametrize the odd ground state using the above PTP  $|e_t\rangle$  of the even ground state and the above parametrization  $\hat{d}_{o\leftarrow e,t}^\dagger$  of the zero-energy excitation:

$$|o_t\rangle := \hat{d}_{o\leftarrow e,t}^\dagger |e_t\rangle \quad (4.8)$$

At this point, it is unknown if  $|o_t\rangle$  is a PTP or not. We anticipate that it is.

#### 6. Proof of proposition 1, step 2.

During the braiding process, the Majorana eigenvector  $\psi_{1t}$  localized at the left edge of the wire is deformed continuously. By the end of the process, it ends up at the right edge, fulfilling either  $\psi_{1T} = \psi_{20}$  or  $\psi_{1T} = -\psi_{20}$ . Similarly,  $\psi_{2T} = \psi_{10}$  or  $\psi_{2T} = -\psi_{10}$ . These possibilities provide 4 possible scenarios for the parametrization of the zero-energy fermionic excitation:

$$\hat{d}_{o\leftarrow e,T}^\dagger = \frac{1}{\sqrt{2}}(\hat{\gamma}_{20} - i\hat{\gamma}_{10}) = e^{-i\pi/2}\hat{d}_{o\leftarrow e,0}^\dagger, \text{ or} \quad (4.9)$$

$$\hat{d}_{o\leftarrow e,T}^\dagger = \frac{1}{\sqrt{2}}(-\hat{\gamma}_{20} + i\hat{\gamma}_{10}) = e^{i\pi/2}\hat{d}_{o\leftarrow e,0}^\dagger, \text{ or} \quad (4.10)$$

$$\hat{d}_{o\leftarrow e,T}^\dagger = \frac{1}{\sqrt{2}}(\hat{\gamma}_{20} + i\hat{\gamma}_{10}) = e^{i\pi/2}\hat{d}_{o\leftarrow e,0}^\dagger, \text{ or} \quad (4.11)$$

$$\hat{d}_{o\leftarrow e,T}^\dagger = \frac{1}{\sqrt{2}}(-\hat{\gamma}_{20} - i\hat{\gamma}_{10}) = e^{-i\pi/2}\hat{d}_{o\leftarrow e,0}^\dagger. \quad (4.12)$$

Importantly, the scenarios (4.9) and (4.10) are ruled out, since  $\hat{d}_T^\dagger$  creates the odd-fermion-parity ground state from the even-fermion-parity ground state, whereas  $\hat{d}_0$  does it the other way around, and latter cannot be obtained by a continuous deformation of the former.

#### 7. Proof of proposition 1, step 3. $|o_t\rangle$ is also a PTP.

$$\langle o_t | \partial_t | o_t \rangle = \langle e_t | \hat{d}_t \partial_t \hat{d}_t^\dagger | e_t \rangle = \langle e_t | \hat{d}_t \left( \partial_t \hat{d}_t^\dagger \right) | e_t \rangle + \langle e_t | \hat{d}_t \hat{d}_t^\dagger \partial_t | e_t \rangle \quad (4.13)$$

The second term vanishes due to  $\langle e_t | \hat{d}_t \hat{d}_t^\dagger \partial_t | e_t \rangle = \langle \hat{d}_t \hat{d}_t^\dagger e_t | \partial_t | e_t \rangle = \langle e_t | \partial_t | e_t \rangle = 0$ . Therefore, by adding  $0 = \langle e_t | \left( \partial_t \hat{d}_t^\dagger \right) \hat{d}_t | e_t \rangle$  to Eq. (4.13), we obtain

$$\langle o_t | \partial_t | o_t \rangle = \langle e_t | \left\{ \hat{d}_t, \left( \partial_t \hat{d}_t^\dagger \right) \right\} | e_t \rangle = \frac{1}{2} \langle e_t | \{ \hat{\gamma}_{At} + i \hat{\gamma}_{Bt}, (\partial_t \hat{\gamma}_{At} - i \partial_t \hat{\gamma}_{Bt}) \} | e_t \rangle = 0. \quad (4.14)$$

In the last step, we used the facts that

$$\{ \hat{\gamma}_{At}, \partial_t \hat{\gamma}_{At} \} = \partial_t \hat{\gamma}_{At}^2 = 0, \quad (4.15)$$

and that

$$\{ \hat{\gamma}_{At}, \partial_t \hat{\gamma}_{Bt} \} = 0, \quad (4.16)$$

since the two Majorana eigenvectors are localized at different edges of the wire.

Eq. (4.14) proves that the parametrization  $|o_t\rangle$  is also a PTP.

8. Proof of proposition 1, step 4. Evaluation of the relative Berry phase.

$$\begin{aligned} \langle o | o(T) \rangle \langle e(T) | e \rangle &= \langle o | o_T \rangle \langle e_T | e \rangle = \langle e | \hat{d}_0 \hat{d}_T^\dagger | e_T \rangle \langle e_T | e \rangle \\ &= e^{\pm i\pi/2} \langle e | \hat{d}_0 \hat{d}_0^\dagger | e_T \rangle \langle e_T | e \rangle = e^{\pm i\pi/2} \end{aligned} \quad (4.17)$$

### 4.3 Cyclic adiabatic non-braiding process in a Kitaev wire

*Proposition:* a non-braiding cyclic adiabatic process in a long topological Kitaev wire results in a relative Berry phase of 0 or  $\pi$  between the even and odd ground states.

### 4.4 Evaluation of the relative Berry phase using the BdG Hamiltonian

1. *Proposition:*  $\psi_{o \leftarrow e, t}$  is a parallel-transport parametrization.

The chosen edge-localized-Majorana-based parametrization of the BdG eigenvector  $\psi_{o \leftarrow e, t}$ , which defines the even-to-odd fermionic excitation  $\hat{d}_{o \leftarrow e, t}^\dagger$ , we have

$$\psi_{o \leftarrow e, t} = \frac{1}{\sqrt{2}} \left[ \begin{pmatrix} \vec{u}_{1t}^* \\ \vec{u}_{1t} \end{pmatrix} + i \begin{pmatrix} \vec{u}_{2t}^* \\ \vec{u}_{2t} \end{pmatrix} \right]. \quad (4.18)$$

A direct calculation resulting in

$$\langle \psi_{o \leftarrow e, t} | \partial_t | \psi_{o \leftarrow e, t} \rangle = 0 \quad (4.19)$$

proves the proposition; one has to invoke  $\partial_t \langle \psi_{o \leftarrow e, t} | \psi_{o \leftarrow e, t} \rangle = 0$  and the spatial localization of the Majorana eigenvectors.

2. Consequence: the relative Berry phase  $\gamma_r$  is the Berry phase picked up by  $\psi_{o \leftarrow e, t}$ .
3. Consequence: the BdG Hamiltonian can of course be used to determine the Berry phase of  $\psi_{o \leftarrow e, t}$ , and therefore to determine the relative Berry phase  $\gamma_r$ .
  - (a) Case 1: no ‘numerical degeneracy’, that is, the numerical diagonalization of the BdG Hamiltonian provides nonzero eigenvalues and therefore provides a single  $\psi$ , and hence – if the ground-state parity is also monitored via the Pfaffian of the BdG matrix – identifies the even-to-odd fermionic excitation.  
When calculating the Berry phase, one has to monitor the parity of the ground state, e.g., using the Pfaffian of the BdG Hamiltonian.
  - (b) Case 2: ‘numerical degeneracy’, that is, the numerical diagonalization of the BdG Hamiltonian provides 2 zero eigenvalues, two corresponding eigenvectors  $\psi_1$  and  $\psi_2$ . Since these are not necessarily fermionic, their appropriate even-to-odd fermionic linear combination  $\psi$  has to be identified.
4. Exercises: calculate/compute the relative Berry phase using the BdG formalism, for the exercises of the 2nd meeting.

**perhaps this is not needed** The BdG Hamiltonian reads

$$\mathcal{H} = \begin{pmatrix} h & \Delta \\ -\Delta^* & -h^* \end{pmatrix} \quad (4.20)$$

$$h = \begin{pmatrix} \epsilon_1 & 0 & t_{13} & 0 \\ 0 & \epsilon_2 & t_{23} & 0 \\ t_{13} & t_{23} & 0 & t_{34} \\ 0 & 0 & t_{34} & \epsilon_4 \end{pmatrix}, \quad (4.21)$$

$$\Delta = \begin{pmatrix} 0 & 0 & \Delta_{13} & 0 \\ 0 & 0 & \Delta_{23} & 0 \\ -\Delta_{13} & -\Delta_{23} & 0 & \Delta_{34} \\ 0 & 0 & -\Delta_{34} & 0 \end{pmatrix}, \quad (4.22)$$

## 4.5 Non-abelian exchange statistics of Majoranas

Two electrons with the same spin: antisymmetric spatial wfn; braiding (adiabatic exchange) results in a Berry phase of  $\pi$ .

Two zero-spin bosons: symmetric spatial wfn, braiding (adiabatic exchange) results in a Berry phase of zero.

These are "abelian" in the sense that if we have more than two particles, then the ordering of exchanging them does not change the final Berry phase.

Here: adiabatic exchange of "Majoranas" results is non-abelian: ordering of exchange matters

Example setup and process [figure]. Consider the two-wire T-junction setup with six sites and four Majoranas. (Generalizable to long Kitaev chains.) The ground state is fourfold degenerate. Take the two-dimensional even ground-state subspace. We choose our basis according to the following principles. We use localized Majorana operators  $\hat{\gamma}_1, \hat{\gamma}_2, \hat{\gamma}_3, \hat{\gamma}_4$ , construct

$$\hat{d}_L = \tag{4.23}$$

$$\hat{d}_R = \tag{4.24}$$

and  $|00\rangle$  denotes the even GS for which  $\hat{d}_L |e_L e_R\rangle = 0$  and  $\hat{d}_R |e_L e_R\rangle = 0$ . Furthermore, we define

$$\hat{d}_L^\dagger |e_L e_R\rangle = |o_L o_R\rangle, \tag{4.25}$$

etc.

The propagator describing a certain adiabatic cyclic process within the even subspace spanned by  $|e_L e_R\rangle$  and  $|o_L o_R\rangle$  is a 2x2 unitary matrix. We want to demonstrate that „the Majoranas show non-abelian exchange statistics”. Within our example, that is exemplified by the following facts.

1. Braiding Majoranas 1 and 2 clockwise results in a propagator

$$U_{12} \equiv \begin{pmatrix} 1 & 0 \\ 0 & e^{-i\pi/2} \end{pmatrix}. \tag{4.26}$$

2. Braiding Majoranas 2 and 3 clockwise results in a propagator

$$U_{23} = \begin{pmatrix} -i & 1 \\ 1 & -i \end{pmatrix}. \tag{4.27}$$

3.  $[U_{12}, U_{23}] = \frac{1}{\sqrt{2}} \begin{pmatrix} 0 & 1+i \\ 1-i & 0 \end{pmatrix} \neq 0$ , and that is referred to as *non-Abelian exchange*.

Calculate  $U_{12}$ .

The braiding process is localized to the left wire. That implies that  $\hat{d}_L^\dagger \hat{d}_L$  commutes with the Hamiltonian during the whole process. Therefore, at the end of the braiding process,  $|e_L e_R\rangle$  arrives into  $e^{i\gamma_{ee}} |e_L e_R\rangle$  and  $|o_L o_R\rangle$  arrives into  $e^{i\gamma_{oo}} |o_L o_R\rangle$ .

### 4.5.1 outdated?

$\begin{pmatrix} \vec{u}^* \\ \vec{v}^* \end{pmatrix}$ : Majorana eigenvectors  $\hat{d}$ : Majorana operators.

Non-abelian exchange statistics of the edge-localized Majorana eigenvectors: noncommuting braiding propagators in a two-wire setup

## 4.6 Majorana qubit

Define Majorana qubit (two wires).

A Majorana qubit is robust as a quantum memory and as a quantum processor.

Explain universal gate set.

Topologically protected operations do not provide a universal gate set.

### .1 The Asbi conjecture and a counterexample

Asbi conjecture: Consider a cyclic adiabatic process of a „superconductor”, that is, of a fermionic Hamiltonian that is quadratic in the creation-annihilation operators. Consider two energy eigenstates  $|1\rangle$  and  $|2\rangle$  that (i) evolve into themselves during the process, up to a Berry phase each,  $\gamma_1$ ,  $\gamma_2$ , and differ by a single-particle excitation  $|2\rangle = \hat{d}^\dagger |1\rangle$ , where  $\hat{d} \equiv \begin{pmatrix} \vec{u}^* \\ \vec{v}^* \end{pmatrix} = \psi$ . The two Berry phases can be different, and the relative Berry phase is defined as  $\gamma_r = \gamma_2 - \gamma_1$ . The conjecture is that the relative Berry phase  $\gamma_r$  equals the Berry phase  $\gamma_\psi$  associated to the BdG eigenvector  $\psi$ .

Show that the conjecture is false, using the  $2\pi$  phase rotation process of the two-site Kitaev chain in the fully dimerized limit. The Hamiltonian is

$$H = c_1^\dagger c_2 + c_2^\dagger c_1 + e^{i\varphi} c_1^\dagger c_2^\dagger + e^{-i\varphi} c_2 c_1, \quad (28)$$

and the cyclic adiabatic process is that  $\varphi$  is tuned from 0 to  $2\pi$ .

1. Determine the 4 instantaneous Fock-space energy eigenvectors: the even ground state  $|e\rangle$ , the odd ground state  $|o\rangle$ , the even excited state  $|e'\rangle$  and the odd excited state  $|o'\rangle$  as functions of  $\varphi$ . Determine the corresponding energy eigenvalues.
2. Show that the relative Berry phase of  $|e\rangle$  and  $|o'\rangle$  is  $\gamma_r = \pi$ .
3. Construct the BdG Hamiltonian.
4. Determine the excitation energy  $E$  and BdG eigenvector  $\psi = \begin{pmatrix} \vec{u}^* \\ \vec{v}^* \end{pmatrix}$  of the single positive-energy excitation  $\hat{d}^\dagger$  as functions of  $\varphi$ . (Mathematica or SymPy or WolframAlpha can help.)

5. Calculate the Berry phase associated to  $\psi$  and compare it to the relative Berry phase calculated above.
6. Optional extra exercise: Show that the positive-energy excitation  $\hat{d}^\dagger$  maps  $|e\rangle$  to  $|o'\rangle$ , that is,

$$|\langle o' | \hat{d}^\dagger | e \rangle| = 1. \quad (29)$$

*Time evolution and the BdG Hamiltonian for adiabatic dynamics.*

1. *Conjecture:* Consider two energy eigenstates  $|n\rangle$  and  $|m\rangle$ , the latter containing an extra positive-energy single-particle excitation with respect to the former,  $|m\rangle = \hat{d}^\dagger |n\rangle$ . The excitation operator is associated to an eigenvector  $\begin{pmatrix} \vec{u} \\ \vec{v} \end{pmatrix}$  of the BdG Hamiltonian. Then, the relative Berry phase  $\gamma$  picked up by the state  $|n\rangle$  and  $|m\rangle$  during a cyclic adiabatic process is the same as the Berry phase picked up by the BdG eigenvector during the same process.
2. *Plan:* counter-examples could be found using analytical or numerical examples. The positive-energy condition can be especially helpful, since that suggests that the excitation is delocalized, and hence the localization argument of the zero-energy version of the statement cannot be invoked.
3. *2-site Kitaev chain in the fully dimerized limit disproves the conjecture.* That provides a counter-example indeed. It can be calculated that the Berry phase associated to the single positive-energy excitation of this model is zero. However, this excitation takes, e.g.,  $|e\rangle$  to  $|g'\rangle$ , the even ground state to the odd excited state, and their relative Berry phase is  $\pi$ . This counter-example disproves the conjecture.

## .2 Quantum-state transfer from a charge qubit to a topological qubit